THERMAL CHARACTERIZATION OF BAUXITE SAMPLES

M. Laskou[1], G. Margomenou-Leonidopoulou[2] and V. Balek[3]*

[1]Department of Geology and Geoenvironment Section of Mineralogy and Petrology, Athens University, Greece
[2]Arkadiou 8, Holargos, 155 62 Athens, Greece
[3]Nuclear Research Institute Řež plc., 250 68 Řež, Czech Republic

Thermal behavior of three characteristic samples from the lower bauxite horizon from locality of Atalandi, Locrida area (Greece) was investigated in the temperature range 20–1250°C by means of emanation thermal analysis (ETA) as well as simultaneous DTA and TG/DTG. The major elements of the samples and the chemical composition of the samples were determined. Moreover, X-ray diffraction was used to characterize the mineralogical composition. It was found that the samples are mainly composed of diaspore, boehmite, gibbsite, kaolinite, hematite, goethite, anatase, chamosite, chloritoid and REE minerals. Differences in chemical and mineralogical composition were observed.

Keywords: bauxite minerals, chemical composition, DTA, ETA, TG/DTG, thermal behavior, XRD

Introduction

The Greek bauxite deposits are included in the Mediter-ranean karst bauxite belt. They are hosted within car-bonate rocks and have been created during four different geological ages. The studied bauxite deposits from the areas of Atalandi (Elatia, Profiti Ilia and Anthochorio) belong to the Subpelagonian zone and lie between Kimmeridian and Triassic limestones [1, 2].

Three representative, typical samples from these deposits were investigated and analyzed with the aim to obtain detailed mineralogical and chemical data about the distribution of major elements in the bauxite samples. The emanation thermal analysis (ETA), and simultaneous DTA, TG/DTG measurements were car-ried to obtain information about the thermal behavior of the three bauxite samples. Moreover, X-ray diffrac-tion was used to obtain the qualitative information about the minerals. The purpose of this paper is to characterize chemical, structural, morphological and textural properties of the typical bauxite samples from localities in Greece.

Experimental

The samples were chemically analyzed and the major elements were determined at XRAL Laboratories, Can-ada. The simultaneous TG/DTG and DTA measure-ments were carried out using Derivatograph D-1500 equipment of the Hungarian Optical Works. Pulverized samples were heated in the range 20–1300°C, at a heat-ing rate of 10°C min^{-1} under static atmospheric condi-tions. Alumina was used as reference. X-ray diffraction patterns were obtained at the University of Athens by using a Philips PW 1010 and CoK$_\alpha$ radiation. The elec-tron micro-probe analyses were carried out at the Uni-versity of Athens, using the Oxford ISIS 300 Energy Depressive System attached to a JEOL JSM-5600 SEM with the following operating conditions: accelerating voltage 20 kV, beam current 0.5 nA, lifetime 50 s, and a beam diameter of 1–2 μm.

The simultaneous ETA and DTA measurements were carried out at the heating rate of 5 K min^{-1}, and air flow of 50 mL min^{-1} using a Netzsch ETA-DTA 404 equipment at Nuclear Research Institute, Řež.

Emanation thermal analysis

In ETA [3–5] the radon released from samples was used to monitor changes of solid surfaces and microstructure of subsurface layers under, in situ con-ditions of heating. This method was already used in the charaterization of the thermal behaviour of kaolinite, montmorillonite, boehmite, kaolinite, vermiculite, saponite, hektorite and other clay minerals and brought about an information about the microstructure devel-opment and surface area changes under in situ heating of the samples [6–10]. The samples for ETA were la-beled by the deposition of drops of acetone solution that contained ^{228}Th and ^{224}Ra as parent nuclides of ^{220}Rn. Atoms of ^{220}Rn were formed from ^{228}Th and ^{224}Ra atoms by spontaneous α-decay and introduced into the subsurface of the sample owing to recoil en-ergy (85 keV per atom). The maximum penetration depth of radon atoms was supposed to be 80 nm, as cal-

culated by Monte Carlo method using TRIM code [11]. The ETA results are expressed as the ratios of the rate of radon release rate to the rate of radon formation in the solid, determined as E (in relative units) $E=A_\alpha/A_{total}$, where A_α is the α-radioactivity of radon released in unit time from the labeled sample, and A_{total} is the total γ-radioactivity of the sample. The A_{total} value is proportional to the rate of radon formation in the sample. Semiconductor and NaI(Tl) detectors are used for the α- and γ-radioactivity measurements, respectively.

Results

Chemical and mineralogical data

Tables 1–3 of this study summarized the geochemistry results of major elements and the results of microanalyses (in mass%), of the main minerals in the three bauxite samples Elatia (denoted as EL), Profitis Ilias (denoted as PI) and Anthochorio (denoted as AN) bauxite samples.

Elatia sample

Mineralogical investigations of this sample indicated that the main minerals are goethite, diaspore and chamosite. Other minerals like hematite, anatase, zircon

and REE minerals are also present in minor amounts. The excess of TiO_2 in diaspore, goethite and hematite is due to a mixture of fine grained anatase. The dominant aluminium mineral in the EL sample is diaspore. The iron content in it varies from 1 to 7 mass%.

The results of the electron microprobe generally showed that the aluminium content in goethite and hematite also varies within the deposit from 1 to 9 mass%.

Profitis Ilias sample

Mineralogical investigations of this sample indicated that the main minerals are diaspore, goethite, hematite, anatase and gibbsite. Other minerals like chamosite and barite are also present in minor amounts.

The dominant aluminium mineral in the PI sample is diaspore. Generally the excess of TiO_2 in diaspore ranges from 0.80 to 3.80 mass% and it is due to the mixture of submicroscopic and fine grained anatase. The electron microprobe results of hematite and goethite generally showed Al contents from 2 to 5 mass%.

Anthochorio sample

Mineralogical investigations of this sample indicated that the main minerals are boehmite, hematite, anatase and goethite. Other minerals like kaolinite,

Table 1 Whole-rock and electron microprobe analyses of the main minerals from the EL sample

	SiO_2	Al_2O_3	Fe_2O_3	MgO	CaO	Na_2O	K_2O	TiO_2	MnO	P_2O_5	L.O.I.*	Total
sample	1.27	11.34	74.58	0.13	0.04	0.04	0.06	0.29	0.04	0.08	12.14	100.01
goethite	3.45	9.19	74.23		0.29			1.59			11.25	100.00
diaspore	1.07	75.30	7.19					1.42			15.02	100.00
chamosite	21.50	24.51	40.50	1.17	0.30		0.36	0.44			11.22	100.00

*calculated

Table 2 Whole-rock and electron microprobe analyses of the main minerals from the PI sample

	SiO_2	Al_2O_3	Fe_2O_3	MgO	CaO	Na_2O	K_2O	TiO_2	MnO	P_2O_5	L.O.I.*	Total
sample	1.59	54.73	24.77	0.03	0.13	0.04	0.03	5.06	0.00	0.07	13.96	100.41
diaspore	1.53	69.53	3.83	0.23				1.27			23.61	100.00
goethite	2.23	2.21	71.55	0.48					0.29		23.24	100.00
chamosite	21.46	21.98	34.37		0.19	1.40	0.79	0.61		0.68	18.52	100.00

*calculated

Table 3 Whole-rock and electron microprobe analyses of the main minerals from the AN sample

	SiO_2	Al_2O_3	Fe_2O_3	MgO	CaO	Na_2O	K_2O	TiO_2	MnO	P_2O_5	L.O.I.*	Total
sample	3.86	49.91	30.18	0.13	0.07	0.00	0.04	3.09	0.12	0.05	12.61	100.06
boehmite	0.50	75.85	6.42					1.77			15.42	100.00
goethite	3.39	2.20	77.87	0.84							15.70	100.00
chamosite	19.27	20.44	46.52	2.38	0.52			0.48		0.44	9.95	100.00

*calculated

chloritoid, chamosite, gibbsite, zircon and REE minerals, are also present in minor amounts.

The dominant aluminium mineral in the AN sample is boehmite. Generally the excess of TiO_2 in boehmite ranges from 0.80 to 1.77 mass% and it is due to the mixture of submicroscopic and fine grained anatase. Electron microprobe results of hematite and goethite generally show Al contents from 0.80 to 2.80 mass%.

Thermal analysis data

DTA and TG/DTG results

The thermal analysis results depend on the paragenesis of the characteristic minerals of the samples. TG/DTG and DTA curves were used to observe the reactions taking place during the thermal treatment of these three samples. Semi-quantitative estimation of the amount of the different minerals present in the sample was made by measurements of the TG/DTG. Figure 1 depicts an overview of DTA, DTG and TG results of the three bauxite samples. The DTA endothermic peaks of the first sample shows goethite (the main endothermal effect at 360°C) was accompanied by the endothermal effects of chamosite (maximum at 520°C), and diaspore (maximum at 545°C). It followed from Fig. 1 that in the second sample gibbsite (endothermal effect at 280°C) and goethite (endothermal effect at 320°C) were accompanied by diaspore (main endothermal effect 545°C). Moreover from Fig. 1 it is obvious that in the third sample the goethite (the endothermal effect

at 360°C) and the main peak of boehmite endothermal effect (maximum at 556°C) are accompanied by an exotherm of kaolinite (maximum at 1080°C). The interpretation of the thermal analysis results in Fig. 1 is based on the general knowledge that the single dehydroxylation endotherm of boehmite (γ-AlOOH) is at about 555°C. The dehydration of its polymorphic phase, diaspore (α-AlOOH), shows a similar endothermic effect, to be ascribed to the decomposition of the sample and the formation aluminium oxide and water, at the temperature near to 545°C. The temperature range of the dehydroxylation was reported [12] to take place between 490 and 580°C. The calculation of the mass loss by using the results of TG/DTG curves demonstrated the diaspore was present in the investigated samples in the different amounts, namely: 3.80 mass%, in the sample denoted EL and 78.51 mass% in the PI sample. The amount of boehmite in the sample denoted AN was 56.00 mass%. It has been determined that boehmite converts into 'transition aluminas' up to 600°C, and at higher temperatures (1100°C) converts to alumina (α-Al_2O_3) with the corundum structure. This transformation temperature varied with boehmite's crystallite size [13, 14].

In the sample denoted PI endothermic effect of gibbsite [γ-Al(OH)$_3$] is determined only around 280°C, and it was associated by the loss of mass as a result of removal of OH groups from the lattice. This wide influence possibly includes the first two endotherms and is attributed to the formation of boehmite [15], which at higher temperatures (here is not observed), between 500 and 550°C is attributed to
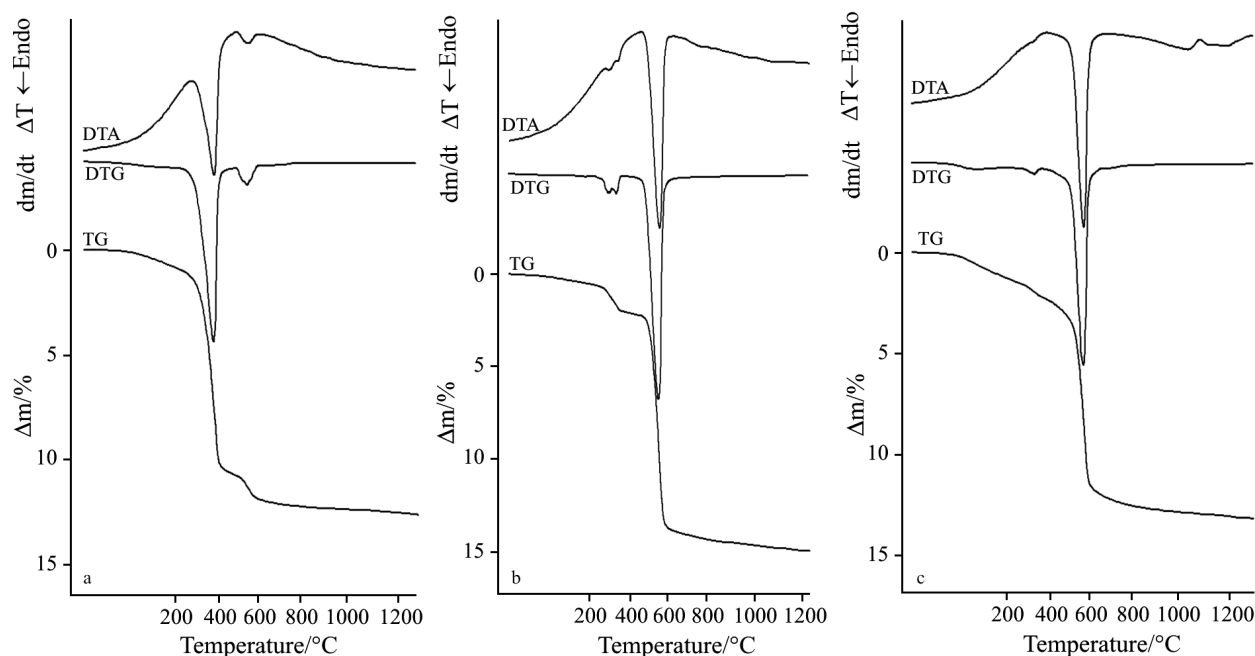

Fig. 1 DTA and TG/DTG curves of Atalandi bauxite samples from a – Elatia (denoted as EL), b – Profitis Ilias (denoted as PI) and c – Anthochorio (denoted as AN)

the dehydroxylation of the earlier formed boehmite to form γ-alumina [16]. The quantitative participation is 2.00 mass% in the sample.

The thermal dehydration effect of Al-goethite [α-(Fe,Al)OOH] was characterized by a mass loss in the range 320 or 360°C, resulting after of the removal of OH groups. The temperature range of the DTA endothermic peak that correspond to the mentioned process was reported between 250 and 360°C [12]. The TG/DTG curves show the quantitative participation of goethite in 83.90, 6.90 and 6.90 mass% in the three samples correspondingly. Goethite contains appreciable aluminium as an isomorphous substitution. This substitution influences the incorporation of non-stoichiometric hydroxyl units in the goethite structure and during thermal dehydroxylation this Al-goethite alters to hydrohematite [17].

In the AN examined samples the exothermic peak is recorded in the temperature of 1080°C. One can suppose that this transformation is in connection with the presence of kaolinite. Formation of metakaolinite which takes place from 530 to 700°C, leads to a wide peak of boehmite. The thermal treatment of kaolinite at a temperature of above 980°C results in the formation of amorphous SiO_2. The recrystallization of mullite occurred when the temperature exceeded 1100°C. Quartz keeps unchanged below 1200°C [18]. The quantitative participation of kaolinite is calculated at 9.40 mass% in the sample.

The dehydroxylation reaction of chamosite is recorded only in the EL sample and in the temperature of 510°C, and its quantitative participation is calculated at 9.28 mass%. This reaction is not obvious in the other samples because it is overlapped by the wide peak of the Al-rich mineral (diaspore or boehmite). The hydroxylation temperatures of Fe^{2+}-rich chlorites are near 450°C and of Mg-rich near 640°C. So the substitution with Mg in our samples (Tables 1–3) guides the dehydration temperature in intermediate values [19].

We can also remark a tendency in the DTA curves of all samples to record exothermic peaks in the range of 350 to 500°C, approximately. It is possible that the oxidation of the organic material which is in the form of organo-mineral complexes created this exotherm [20].

ETA results

ETA made it possible to characterize the microstructure development of the samples under in situ conditions of heating. The ETA results of the three bauxite samples measured at identical conditions are presented in Fig. 2 to characterize the differences in their thermal behavior and to compare the microstructure development of the samples on heating.

In the interpretation of the ETA data it was supposed [3, 4] that radon atoms were released from the labelled sample by two processes, namely (*i*) by the recoil of radon atoms formed by spontaneous α-decay of radium and/or (*ii*) by diffusion of trapped radon atoms at lattice defects, such as vacancy clusters, grain boundaries and pores. The emanation rate, *E*, can be expressed in a simplified way as [3]

$$E = E_R + E_D = S[K_1 + (D/\lambda)^{1/2} K_2]$$

where E_R is the part of the radon release due to recoil, E_D is the diffusion part of the released radon, *S* is the surface area, K_1 is the temperature independent constant, proportional to the penetration depth of radon recoil atoms, *D* is the coefficient of radon diffusion in the sample, λ is the decay constant of radon, and K_2 is a constant dependent of temperature. Consequently, the increase in the emanation rate (*E*) can be due to the structure loosening i.e. opening of the structural channels, formation of crakes or pores, etc. and/or to an increase in the surface area of the interfaces. On the other hand, the decrease in *E* reflected the annealing of structure irregularities serving as paths for radon migration, densification of structure, closing pores, sintering, and/or a decrease in the surface area of the interfaces.

ETA results of the three bauxite samples measured during heating in air are presented in Fig. 2. Curve 1 corresponds to the sample denoted EL, curve 2 to the sample denoted PI and curve 3 to the sample denoted AN.

By using the ETA results we have determined the temperature intervals and changes of surface area due to the thermal decomposition of the individual components of the samples. Moreover, from the decrease of the emanation rate, *E*, the decrease of surface area of the samples was indicated.

The dehydroxylation of goethite, diaspore or boehmite was characterized by the increase in the radon release rate *E*(*T*). The increase of *E*(*T*) observed in Fig. 2 can be ascribed to the thermal degradation of
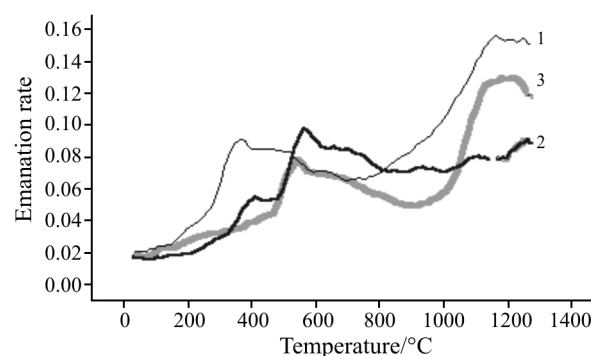

Fig. 2 Comparison of the ETA results of the bauxite samples measured during heating in air to 1300°C; curve 1 corresponds to the sample denoted EL, curve 2 to the sample denoted PI and curve 3 to the sample denoted AN

mainly diaspore (curve 2), goethite (curve 1) and boehmite (curve 3). It was assumed that the radon diffusion by volume mechanism enhanced the increase of the radon release rate on heating above 900°C. As it followed from Fig. 2 the increase of $E(T)$ was more intense the case of the goethite-rich sample than for the boehmite-rich sample. The diaspore-rich sample was characterized by lower slope the $E(T)$ increase. We supposed that these differences are due to the differences in the mineralogical composition of the samples and particularly to their structural morphological and textural properties, and it was confirmed by DTA results [16–20].

At elevated temperatures above 1100°C, where no changes of the mass were observed, the decrease of the radon release rate, E, indicated sintering of the samples. The decrease of the $E(T)$ was assumed to be proportional to the relative sinterability of the pre-ceramic powders that resulted after thermal decomposition of bauxite minerals.

Conclusions

- Thermal analysis methods – DTA, TG/DTG and ETA characterized the thermal behavior of three bauxite samples from the localatity Atalandi, Greece. The differences in the thermal behavior of the bauxite samples observed are in accordance with the content of the individual minerals present in the samples. Goethite is the principal mineral in EL with chamosite. Diaspore is the main mineral in PI sample with chamosite. AN sample was characterized by an abundance of boehmite and in addition the presence of kaolinite and chloritoid.
- The aluminium content in goethite varies within each deposit. For the sample from Elatia, for Al_2O_3 content 9.19 mass% the dehydroxylation temperature of goethite is 360°C. For the sample from PI, for Al_2O_3 content 2.21 mass% the dehydroxylation temperature of goethite is 320°C and similarly for the sample from Anthochorio, for Al_2O_3 content 2.20 mass% the dehydroxylation temperature of goethite is 330°C. Consequently it can be concluded that there is a connection between the decomposition temperature of goethite and the extent of the substitution of iron by aluminium in the examined samples.
- The content of iron in diaspore or boehmite varied in the samples within each deposit up to 7 mass%.

References

1 G. Maratos, Bull. Geol. Soc. Greece, V/1 (1962) 29.
2 M. Laskou, F. Paulik and J. Paulik, Travaux du Comité International pour l'étude des Bauxites de l' Alumine et de l' Aluminium, 13/18 (1983) 73.
3 V. Balek, Thermochim. Acta, 192 (1991) 1.
4 V. Balek, J. Šubrt, T. Mitsuhashi, I. N. Beckman and K. Györyová, J. Therm. Anal. Cal., 67 (2002) 15.
5 V. Balek and J. Tölgyessy, Wilson and Wilson's Comprehensive Analytical Chemistry, Part XIIC, G. Svehla, Ed., Elsevier Science Publishers, Amsterdam 1984, p. 304.
6 V. Balek and M. Murat, Thermochim. Acta, 282–283 (1996) 385.
7 J. Poyato, L. A. Perez-Maqueda, M. C. Jimenez de Haro, J. L. Perez Rodriguez, J. Šubrt and V. Balek, J. Therm. Anal. Cal., 67 (2002) 73.
8 V. Balek, Z. Malek, S. Yariv and G. Matuschek, J. Therm. Anal. Cal., 56 (1999) 67.
9 V. Balek, J. Šubrt, J. Rouquerol, P. Llewellyn, V. Zelenák, I. M. Bountsewa, I. N. Beckman and K. Györyová, J. Therm. Anal. Cal., 71 (2003) 773.
10 L. A. Perez-Maqueda, V. Balek, J. Poyato, J. L. Perez Rodriguez, J. Šubrt, I. M. Bountsewa, I. N. Beckman and Z. Malek, J. Therm. Anal. Cal., 71 (2003) 715.
11 J. F. Ziegler and J. P. Biersack, The Stopping and Range of Ions in Solids, Pergamon Press, New York 1985.
12 D. N. Todor, Thermal Analysis of Minerals, Abacus Press, Kent 1976.
13 P. Souza Santos, H. Souza Santos and S. P. Toledo, Mater. Res., 3/4 (2000) 104.
14 X. Bokhimi, J. A. Toledo-Antonio, M. L. Guzman-Castillo and F. Hernandez-Beltran, J. Solid State Chem., 159 (2001) 32.
15 F. Paulik, J. Paulik and L. Erdey, Anal. Chim. Acta, 29/5 (1963) 381.
16 W. Smykatz-Kloss, Differential Thermal Analysis (Minerals and Rocks, Vol. 11), Springer-Verlag, Berlin 1974.
17 H. D. Ruan, R. L. Frost, J. T. Kloprogge and L. Duong, Spectrochim. Acta, Part A, 58 (2002) 479.
18 G.-Z. Qiu, T. Jiang, G.-H. Li, X.-H. Fan and Z.-C. Huang, Scandinavian J. Metallurgy, 33 (2004) 121.
19 T.-B. Bai, St. Guggenheim, S.-J. Wang, D. G. Rancourt and A. F. Koster van Groos, Am. Miner., 78 (1993) 1208.
20 S. Yariv, Thermal Analysis in the Geosciences, Vol. 38, W. Smykatz-Kloss and S. St. J. Warne (Eds), Chapter V, Springer-Verlag, Berlin 1991, pp. 328–351.